Fermi-edge singularities in the optical emission of doped direct and indirect quantum wells

1996 J. Phys.: Condens. Matter 8 1713

(http://iopscience.iop.org/0953-8984/8/11/015)

J. Phys.: Condens. Matter **8** (1996) 1713–1728. Printed in the UK

Fermi-edge singularities in the optical emission of doped direct and indirect quantum wells

F J Rodríguez† and C Tejedor‡

† Departamento de Física, Universidad de los Andes, AA 4976, Santafé de Bogotá, Colombia
‡ Departamento de Física de la Materia Condensada, C-XII, Universidad Autónoma de Madrid, Cantoblanco 28049, Madrid, Spain

Received 21 August 1995, in final form 20 November 1995

Abstract. We study the luminescence spectrum of doped direct and indirect quantum wells. The Bethe–Salpeter equation is solved in a three-band model of parabolic wells including a static screened Coulomb interaction. In order to obtain a strong enhancement at the Fermi edge we found that it is necessary to break the symmetry of the system by shifting the electron and the hole confining parabolic potentials with respect to each other. This condition allows for a new scattering mechanism which is responsible for strong enhancements. Taking an infinite mass for the hole we found an increasing signal of the spectrum at the Fermi edge when two conditions are fulfilled: (i) the separation between the electrons and hole gravity centres is of the order of the well width; and (ii) the Fermi edge is close to the bottom of the second conduction subband. The effects of temperature and hole localization are analysed. Satisfactory agreement with recent experimental results is obtained.

1. Introduction

The investigation of a two-dimensional electron gas (2DEG) in modulation-doped quantum wells has recently attracted attention both as regards the fundamental physics and as regards potential device applications [1–6]. The spatial separation between the 2DEGs and the dopants allows one to obtain a high mobility of the electrons and consequently a reduced scattering by impurities. So far, experimental and theoretical studies have concentrated on transport properties. However, optical properties have in recent years received considerable attention from the physics point of view and as regards possible applications in technological devices—for example quantum well lasers [7] and high-electron-mobility transistors [8]. In particular, spectroscopy of doped parabolic quantum wells (DPQW) is of great interest because such systems are quasi-two-dimensional in terms of the Coulomb effects and allow one to observe many-body effects such as: (i) the breakdown of the fractional quantum Hall effect when the width of the electronic layer is increased [9]; (ii) the presence of a strong Fermi-edge singularity (FES) [10–14] due to the multiple electron–hole scattering; and (iii) the existence of shake-up processes [15]. In particular, much of the previous experimental and theoretical work was focused on modulation-doped symmetric quantum wells (in the following, direct systems) where the presence of the FES is discussed in terms of the strong localization of the photoexcited hole [16, 17, 18]. In this case the excitation is performed under low-power excitation so that the photoexcited carriers can be considered as in equilibrium with the Fermi sea of doping-originated electrons, where the electrons and holes coexist in the same spatial region and a strong electron–hole overlap occurs. Due to

0953-8984/96/111713+16$19.50

the symmetry of this system, coupling of the FES with virtual transitions to other conduction subbands cannot be achieved.

Therefore, we are interested in the study of the FES in asymmetric modulation-doped quantum wells (AMDQW) (in the following, indirect systems) where new and interesting experimental results have emerged. Although the wells are no longer parabolic, we can still retain parabolic potentials to describe the lowest states of actual wells. Due to the asymmetry of the confining potential the wavefunctions of different electron subbands have different extensions in real space normal to the plane containing the 2DEG and thus have different overlaps with the hole wavefunction. This large difference in the wavefunction overlaps can result in the presence of any transition from the lowest electron subbands to the hole states when there is more than one electron subband populated. In this case, one of the most striking features is the strong enhancement of the luminescence arising from the Fermi edge [19, 20]. The presence of a FES in symmetric quantum wells has been confirmed by experiments [3, 10, 12, 21] involving localized holes but with a signal at the Fermi level lower than in the asymmetric case. There, strong enhancements appear due to the spatial breaking of the symmetry in the system, with the gravity centres of the wavefunctions for electrons and holes separated by a distance a. The experimental situation shows that the creation of the photohole represents a finite perturbation to the Fermi sea previously in equilibrium. Therefore, these are good systems for which to study many-body problems close to equilibrium situations. For this case we use Feynman diagram techniques, and sum the most divergent terms up to the second order. We found that the ladder approach describes the experimental situation well [4, 11, 12] provided that the finite lifetime of the hole is taken into account. For these asymmetric quantum wells experiments have shown that parameters such as the separation between the bottom of the second subband and the Fermi edge, temperature effects, and the a-separation become important for the optical response of the system at the Fermi edge [4, 12, 22]. Therefore, one of the main objectives of this paper is to study a FES coupled with a resonant state.

By solving numerically the Bethe–Salpeter equation we study the luminescence spectrum of parabolic MDQW for direct and indirect systems. In this case the ladder approximation is valid if we take into account an appropriate screened electron–hole interaction and adequate spectral functions for the hole [13, 16, 18, 23, 24]. It must be pointed that femtosecond pulsed laser experiments in which the photoinduced carriers are far from equilibrium need to be described using more elaborate theories [25, 26]. We will show that the FES intensity can be regulated by changing the separation a of the parabolic potentials confining electrons and holes as well as the intersubband spacing Δ controlled by the curvature of the potentials. When the separation of the hole wavefunction from the 2DEG is approximately of the same order as the width of the well and independent of the intraband spacing, the signal at the Fermi edge increases. This increase is much stronger when the Fermi level is slightly below the bottom of a subband. In this case a new scattering channel couples the transitions between electrons at the Fermi edge through empty states at the bottom of the next subband.

Luminescence spectra are analysed as a function of temperature. For indirect systems a second peak in the emission spectrum appears, due to the electrons thermally excited to the bottom of the next subband. The FES disappears when the temperature reaches approximately 70 K in satisfactory agreement with recent experiments performed on MDQWs [19, 20]

The paper is organized as follows. Expressions for the interacting electron–hole Green function within a ladder approximation and for the appropriate screened electron–hole Coulomb interaction within a random-phase approximation (RPA) are given in section 2. Effects of finite temperature, different electron densities and the hole lifetimes have been

taken into account. In section 3 the numerical results are given and a comparison with the experimental situation is established. Finally, the main conclusions are summarized in section 4.

2. Description of the model

To calculate the optical properties of the Q2D electron gas, we follow the formalism given in [23, 24, 27]. This formalism can be used in systems near to the equilibrium situation in which a thermodynamic basis is well known. The luminescence spectrum for MDQW systems is obtained using the Bethe–Salpeter equation (the ladder approximation) [23, 24, 27, 28]. As has been discussed [24, 27, 29] the ladder approximation does not give good results if the electron–hole interaction and the hole lifetime are not considered appropriately. The summing of ladder diagrams for an on-site interaction can be performed exactly and the emission or absorption at the Fermi level can develop a strong enhancement only if the inverse of the non-interacting electron–hole Green function as a function of frequency intersects the on-site value potential [13, 24, 29]. Then, the spectrum shows a logarithmic divergence at the Fermi level arising from a simple pole in the non-interacting electron–hole Green function instead of a potential divergence as it should. Consequently an on-site interaction cannot be used and it is necessary to take into account an adequate electron–hole interaction, screened by the Fermi sea. Moreover, in order to get an adequate lineshape for the emission spectra, the lifetime of the valence band hole must be considered. This can be included in a consistent form within the ladder approximation by dressing the hole propagator [18, 23, 24]. This produces a power-law divergency at the Fermi level instead of the incorrect logarithmic one. In our model we consider a quasi-2DEG, in which electrons are free to move in the x–y plane, with a harmonic oscillator confinement in the z-direction. In order to simplify the numerical calculations for the Bethe–Salpeter equation, we assume a static screened electron–hole Coulomb interaction. In this way, plasmons satellites arising from electron–electron interactions are not considered here.

Within a ladder approximation the interacting electron–hole Green function for equilibrium systems at finite temperatures can be written, in two dimensions, as

$$\begin{aligned} G_{n_v,n_c;n'_v,n'_c}(\boldsymbol{k},\boldsymbol{k}',\omega) &= G^0_{n_v,n_c;n'_v,n'_c}(\boldsymbol{k},\boldsymbol{k}',\omega) + \frac{1}{A}\sum_{\Gamma'',\Gamma'''} G^0_{n_v,n_c;n''_v,n''_c}(\boldsymbol{k},\boldsymbol{k}'',\omega) \\ &\quad \times V^{(s)}_{n''_v,n''_c;n'''_v,n'''_c}(|\boldsymbol{k}''-\boldsymbol{k}'''|) G_{n'''_v,n'''_c;n'_v,n'_c}(\boldsymbol{k}''',\boldsymbol{k}',\omega) \end{aligned} \tag{1}$$

where $\Gamma'' = [n''_c, n''_v, \boldsymbol{k}'']$, n_v and n_c being the valence and conduction subband indices, respectively, $\boldsymbol{k}''$ is the two-dimensional wavevector and A represents the area of the quantum well. The first term in (1) represents the non-interacting electron–hole Green function given by

$$\begin{aligned} G^0_{n_v,n_c;n'_v,n'_c}(\boldsymbol{k},\boldsymbol{k}',\omega) &= \delta_{n_v,n'_v}\delta_{n_c,n'_c}\,\delta(\boldsymbol{k}+\boldsymbol{k}')\int \mathrm{d}\omega_h\; A_h(-k,\omega_h)\frac{1-n_F(E_e(k))-n_F(E_h(k))}{\omega - E_{n_e}(k)-\omega_h+\mathrm{i}\delta} \end{aligned} \tag{2}$$

where $n_F(E_{e\,(h)}(k))$ is the Fermi distribution for electrons (holes).

The self-energy of the valence band hole is included by dressing the hole propagator through a spectral function $A_h(-k,\omega_h)$. The explicit form of this function has been

discussed previously [18, 24, 30, 31], the only difference arising from the g-factor which depends on the dimensionality through the electron polarizability and the screened Coulomb potential. This term takes into account the rate of creation of electron–hole pairs at the Fermi energy; the explicit form in two dimensions is given later.

In order to use the Bethe–Salpeter equation, we need to calculate the screened Coulomb matrix elements for direct and indirect systems.

2.1. The screened Coulomb interaction

2.1.1. Direct systems. For direct systems, we assume that electrons and holes are confined in the same z-spatial region by parabolic potentials and that they are free to move in the x–y plane. The eigenfunctions for electrons and holes are given by

$$\Psi_{n,k}(\boldsymbol{\rho}, z) = \frac{\mathrm{e}^{\mathrm{i}\boldsymbol{k}\cdot\boldsymbol{\rho}}}{\sqrt{A}}\psi_n(z) \tag{3}$$

where

$$\psi_n(z) = \sqrt{\frac{1}{2^n n!\sqrt{\pi}l}}\mathrm{e}^{-z^2/2l^2}H_n\left(\frac{z}{l}\right).$$

Here n represents the subband index and H_n a Hermite polynomial. We assume that the electrons and holes are characterized by the same characteristic length $l = \sqrt{(\hbar^2/m_e^*\Delta)}$. The free-particle dispersion is assumed to be parabolic, i.e, $E_e(k) = E_g + \hbar^2k^2/2m_e^*$ and $E_h(k) = -\hbar^2k^2/2m_h^*$, where m_e^* and m_h^* represent the effective masses of electrons and holes, respectively, Δ is the characteristic frequency of the harmonic potential confining electrons and E_g is the energy gap. From the wavefunctions of electrons and holes, it is straightforward to get the unscreened Coulomb interaction between them. The bare electron–hole Coulomb interaction in two dimensions reads in general

$$V^{(0)}_{i,j;m,n}(\boldsymbol{k}, \boldsymbol{k}', \boldsymbol{k}'', \boldsymbol{k}''') = -\frac{e^2}{\varepsilon_s}\int \mathrm{d}\boldsymbol{r}_e \int \mathrm{d}\boldsymbol{r}_h \, \frac{\Psi_{i,\boldsymbol{k}}(z_e)\Psi^*_{j,\boldsymbol{k}'}(z_e)\Psi_{m,\boldsymbol{k}''}(z_h)\Psi^*_{n,\boldsymbol{k}'''}(z_h)}{\sqrt{(\boldsymbol{\rho}_e - \boldsymbol{\rho}_h)^2 + (z_e - z_h)^2}} \tag{4}$$

where $\boldsymbol{\rho}_e$ and $\boldsymbol{\rho}_h$ are two-dimensional vectors for electrons and holes in the x–y plane respectively. For $E_F < \Delta$ the effects of higher subbands can be neglected for direct systems. Therefore, only one matrix element of the bare Coulomb interaction has to be calculated, given by

$$V^{(0)}_{0,0;0,0}(q) = -\frac{2\pi}{q}\frac{e^2}{\varepsilon_s}F_{0,0;0,0}(q) \tag{5}$$

where the factor $2\pi e^2/(\varepsilon_s q)$ is the purely 2D Coulomb interaction and $F_{0,0;0,0}(q)$ represents the form factor, which takes into account the effect of confinement from a pure 2D system to the quasi-three-dimensional (Q3D) system,

$$F_{0,0;0,0}(q) = \mathrm{e}^{q^2l^2/2}\left[1 - \Phi\left(\frac{ql}{2}\right)\right]$$

where $\Phi(ql/2)$ is the complementary error function [32] and $q = |\boldsymbol{k} - \boldsymbol{k}'|$ is the relative total momentum. In undoped systems this is the correct potential to use for the electron–hole interaction. If there is a large electron concentration, however, the bare Coulomb potential will be screened by the electrons. This is given in the RPA by the static dielectric constant

$$\epsilon_{0,0;0,0}(q) = 1 - \chi_{0,0}(q)V^{(0)}_{0,0;0,0}(q) \tag{6}$$

with the polarizability function given by

$$\chi_{0,0}(q) = -\frac{m_e^*}{\pi\hbar^2}\begin{cases} 1 & x < 1 \\ 1-\sqrt{1-x^2} & x > 1 \end{cases} \tag{7}$$

with $x = 2k_{F_0}/q$, and where k_{F_0} represents the Fermi momentum in the first subband, $k_{F_0} = (2m_e^* E_F/\hbar^2)^{1/2}$. Note that $\chi_{0,0}(q)$ depends only on q and that $E_F \to 0 \Rightarrow \chi_{0,0}(q) \to 0$ and hence $\epsilon_{0,0;0,0} \to 1$. When considering only s-wave electron–hole scattering, the screened Coulomb interaction is replaced in the Bethe–Salpeter equation by its angle-averaged value

$$V^{(s)}_{0,0;0,0}(k,k') = \frac{1}{2\pi}\int_0^{2\pi} \mathrm{d}\theta\ V^{(s)}_{0,0;0,0}(|\boldsymbol{k}-\boldsymbol{k}'|) \tag{8}$$

where

$$V^{(s)}_{0,0;0,0}(q) = \frac{V^{(0)}_{0,0;0,0}(q)}{\epsilon_{0,0;0,0}(q)} \tag{9}$$

represents the diagonal-matrix screened Coulomb interaction. It must be pointed out that this is only valid if just one conduction subband is occupied by free carriers.

2.1.2. Indirect systems. In this case, we assume that the gravity centre for the hole is displaced in the z-direction a distance a from the 2DEG. This breaking of symmetry provokes the hole potential to couple electron states from different subbands. The eigenfunctions for electrons are the same as for the direct systems. The hole will be characterized by a wavefunction

$$\Psi_0(z-a) = \left[\frac{1}{\sqrt{\pi l^2}}\right]^{1/2} \mathrm{e}^{(z-a)^2/2l^2}. \tag{10}$$

Therefore, we analyse only interactions between first heavy-hole, v, subbands to first, c_1, and second, c_2, conduction subbands. Within this three-band model a new scattering channel is opened and the enhancement of the FES can be explained by the resonant coupling of the states c_1 and c_2

Due to the width of the well in the z-direction the bare Coulomb interaction is reduced by a form factor, which takes into account the confinement in this direction:

$$V^{(0)}_{i,j;m,n}(q,a) = -\frac{2\pi e^2}{\epsilon_s q} F_{i,j;m,n}(q,a) \tag{11}$$

where the form factor is given by the term $F_{i,j;m,n}$ and $i, j; m, n$ represent subband indices. We define the functions

$$\Phi^{(+)} = \Phi\left[\left(q+\frac{a}{l^2}\right)\frac{l}{\sqrt{2}}\right] \qquad \Phi^{(-)} = \Phi\left[\left(q-\frac{a}{l^2}\right)\frac{l}{\sqrt{2}}\right] \tag{12}$$

where $\Phi(x)$ represents the complementary error function [32]. In our case, the form factors of the bare Coulomb elements which play an important role in the enhancement at the Fermi edge are given by intrasubband terms

$$F_{0,0;0,0}(q,a) = \frac{1}{2}\mathrm{e}^{-a^2/2l^2}\left[\mathrm{e}^{(l^2/2)[q+a/l^2]^2}(1-\Phi^{(+)}) + \mathrm{e}^{(l^2/2)[q-a/l^2]^2}(1-\Phi^{(-)})\right] \tag{13}$$

$$F_{0,1;0,1}(q,a) = \left[1+\left(\frac{ql}{\sqrt{2}}\right)^2\right]F_{0,0;0,0}(q,a) - \frac{ql}{\sqrt{2\pi}}\mathrm{e}^{-a^2/2l^2} \tag{14}$$

and intersubband terms

$$F_{0,0;0,1}(q,a) = -ql\frac{1}{2}\mathrm{e}^{-a^2/2l^2}\left[\mathrm{e}^{(l^2/2)[q+a/l^2]^2}(1-\Phi^{(+)}) - \mathrm{e}^{(l^2/2)[q-a/l^2]^2}(1-\Phi^{(-)})\right]. \tag{15}$$

Equations (13)–(15) multiplied by the bare Coulomb interaction in two dimensions represent the electron–hole intrasubband and intersubband elements respectively. Note that for $a = 0$, $F_{0,0;0,1}(q,a) = 0$, so a coupling between the first and second conduction subbands through the hole potential does not occur.

In order to obtain the appropriate screened Coulomb interaction, the dielectric constant of the system has to be found. Due to the asymmetry of the potential, the dielectric constant matrix will become non-diagonal. Depending on whether the second conduction subband is occupied or unoccupied by electrons a new term in the polarizability function appears or does not; it is given by

$$\chi_{0,1}(q) = \begin{cases} 1 & \text{if } x_0 > y_0 \text{ and } x_1 > y_1 \\ 1 - \dfrac{1}{2}\sqrt{y_0 - x_0} & \text{if } x_0 < y_0 \text{ and } x_1 > y_1 \\ 1 - \dfrac{1}{2}\sqrt{y_1 - x_1} & \text{if } x_0 > y_0 \text{ and } x_1 < y_1 \\ 1 - \dfrac{1}{2}\sqrt{y_1 - x_1} - \dfrac{1}{2}\sqrt{y_0 - x_0} & \text{if } x_0 < y_0 \text{ and } x_1 < y_1 \end{cases} \tag{16}$$

where the subband indices 0 and 1 label the first and second electronic subbands respectively, and

$$x_0 = \left(\frac{2k_{F0}}{q}\right)^2 \qquad x_1 = \left(\frac{2k_{F1}}{q}\right)^2$$
$$y_0 = \left(1 + \frac{\Delta}{E_e(q)}\right)^2 \qquad y_1 = \left(1 - \frac{\Delta}{E_e(q)}\right)^2.$$

k_{F0} and k_{F1} represent the Fermi momentum in the first and second conduction subbands, respectively. Note that $\chi_{0,1} = \chi_{1,0}$. With these matrix elements known, we can calculate all screened Coulomb matrix elements (details are given in [31]).

2.2. The hole spectral function

In order to obtain an adequate non-interacting electron–hole Green function, it has been shown [13, 24, 23, 31, 33, 34] that it is necessary to take into account the hole lifetime. This can be calculated if we consider the interactions between the valence band hole and the electron–hole pairs at the Fermi level in a way that is consistent with the ladder approximation. By contrast, for electrons this point is not so important, because electron lifetimes imply broadenings much smaller than the electronic chemical potential. Thus, the electron spectral function is taken as

$$A^e = 2\pi\,\delta(\hbar\omega - E_e(k)). \tag{17}$$

Due to the sudden appearance of the hole, low-energy electron–hole pairs around the Fermi level are generated. The number of these excitations can be calculated as

$$R(\omega) = \frac{1}{4\pi^3}\int \mathrm{d}^2k\,\left[\frac{V^{(0)}_{0,0;0,0}}{|\epsilon(k,0)|}\right]^2\left[-\mathrm{Im}\,\chi_{0,0}(k,\omega)\right] \tag{18}$$

where Im $\chi_{m,n}$ is the imaginary part of the multiband electron polarizability given by

$$\begin{aligned}\operatorname{Im}\chi_{m,n}(q,\omega) &= \frac{m_e^*}{\pi\hbar q}\left\{\left[k_{F_n}^2-\left(\frac{E_q-\hbar\omega-\Delta_{nm}}{\hbar^2 q/m}\right)^2\right]^{1/2}\right. \\ &\left.+\left[k_{F_m}^2-\left(\frac{E_q+\hbar\omega-\Delta_{mn}}{\hbar^2 q/m}\right)^2\right]^{1/2}\right\} \qquad (19)\end{aligned}$$

for $\omega \neq 0$, while $\operatorname{Im}\chi_{m,n}(q,0)=0$. $\Delta_{mn}=E_n-E_m$ represents the electronic intersubband separation. For low-energy excitations $R(\omega)$ is given as a linear function of frequency:

$$R(\omega)=g\omega \qquad (20)$$

where g is given by

$$g=\frac{1}{1+k_F\epsilon\hbar^2/m_e^*e^2} \qquad (21)$$

in two dimensions [30]. The main difference from the one-dimensional case is that now this exponent depends on the electronic density. With this term the hole spectral function A_h can be easily calculated in the same way as for the one-dimensional case [24]. It is important to note that the spectral function needs to be calculated up to second order in the perturbation diagrams in order to be consistent with the ladder approximation. This gives a good lineshape. From this the non-interacting electron–hole Green function can be obtained.

2.3. Interacting electron–hole Green functions

In indirect systems we need to solve a set of Bethe–Salpeter coupled equations. For the case of one hole and two conduction subbands of interest here, we obtain a set of four equations from which all intrasubband and intersubband transitions can be obtained [34]:

$$\begin{aligned}G_{00;00} &= G_{00}^{(0)}+G_{00}^{(0)}V_{00;00}^{(s)}G_{00;00}+G_{00}^{(0)}V_{00;01}^{(s)}G_{01;00}\\ G_{01;00} &= G_{11}^{(0)}V_{01;00}^{(s)}G_{00;00}+G_{11}^{(0)}V_{01;01}^{(s)}G_{01;00}\\ G_{00;01} &= G_{00}^{(0)}V_{00;00}^{(s)}G_{00;01}+G_{00}^{(0)}V_{00;01}^{(s)}G_{01;01}\\ G_{01;01} &= G_{11}^{(0)}+G_{11}^{(0)}V_{00;01}^{(s)}G_{00;01}+G_{11}^{(0)}V_{01;01}^{(s)}G_{01;01}\end{aligned} \qquad (22)$$

where $G_{ij;kl}$ and $G_{ii}^{(0)}$ represent the matrix elements of the interacting and non-interacting electron–hole Green functions respectively. In this set of equations the off-diagonal term $G_{00;01}$ represents the mixing of v–c_1 and v–c_2 transitions and it will be responsible for the enhancement of the FES in the luminescence spectrum. Note that the intersubband propagators $G_{01;00}=G_{00;01}$ in (22) disappear when $V_{00;01}$ or $V_{01;00}$ is equal to zero, i.e., for a direct system. The screened Coulomb interaction component $V_{00;10}^{(s)}$ represents the scattering of a first conduction subband electron by a second subband conduction electron due to the presence of the hole [31].

3. Results and comparison with the experimental situation

Firstly, we analyse the effects arising from the finite mass of the hole in a symmetric system. The parameters used in our calculation are as follows: $\epsilon_s=12$, $m_e^*=0.067m_0$ and the

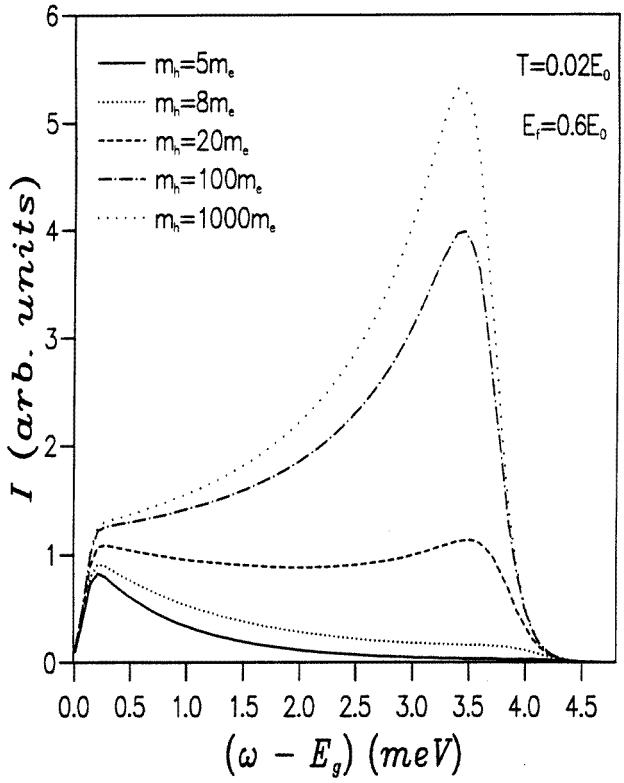

Figure 1. Luminescence spectra for a direct quantum well. The hole mass is varied in units of the electron effective mass m_e^*. $E_F = 3.6$ meV, $\Delta \to \infty$ and $E_0 = 6$ meV. The energy is measured with respect to the quantum well gap E_g.

exciton binding energy $E_0 = 6$ meV. In order to describe the hole mobility, we show in figure 1 the numerical results obtained by solving the Bethe–Salpeter equation with different hole masses. We use the parameters $E_F = 3.6$ meV and $T = 3$ K [35]. We suppose that our system is in the two-dimensional quantum limit, i.e., that the second conduction subband is far away from the Fermi edge ($\Delta \to \infty$), and yet reaches a quasi-equilibrium state. We consider only recombination processes between electrons occupying the first conduction subband and the hole in the valence band.

Of particular interest in figure 1 is the change in the lineshape of the luminescence spectrum when the hole mass goes from $m_h = 5m_e^*$ to $m_h = 1000m_e^*$, i.e. to practically infinity, showing a clear enhancement at the Fermi level. Optical processes must conserve momentum. Now, the luminescence spectrum involves two types of transition in k-space: (1) indirect transitions that recombine electrons at the Fermi level with holes at the top of the valence band, with the simultaneous excitations of electron–hole pairs at the Fermi level which ensure energy and momentum conservation; the minimum energy required for such process is given by $\hbar\omega_i = E_g + E_F$; (2) direct transitions that recombine electrons at the Fermi level with holes with the same momentum. In order to ensure momentum conservation a minimum energy $\hbar\omega_d = E_g + (1 + m_e^*/m_h^*)E_F$ is required as is a momentum $\boldsymbol{k}_F^e = \boldsymbol{k}_F^h$. For a finite effective hole mass, the holes thermalize quickly to the top of the valence band ($\boldsymbol{k}_h = 0$) and so momentum conservation occurs only if the recombination processes occur

with $k_e = 0$. The energy difference between indirect and direct transitions allows the hole relaxation, and all the transitions from the top of the Fermi edge will become broadened. Therefore, a weak FES appears at $\hbar\omega - E_g = (1 + m_e^*/m_h^*)E_F$. As we see in figure 1 the main contribution to the luminescence spectrum arises from electrons at the bottom of the conduction subband ($k_e \approx 0$) (the continuous line). By contrast, if the hole mass is increased, i.e, if the dispersion relation for the hole flattens, the behaviour of the hole is similar to that of a scattering centre for the electrons, and direct transitions are possible. This behaviour is consistent with the fact that no FES was observed in high-quality modulation-doped multiple quantum wells, while they are better observed when some disorder localizes the holes [36, 37]. In figure 1 the washout of the FES in the emission spectrum for the finite-hole-mass case is clearly shown. Then, a FES arises only from electronic correlations at the Fermi edge. Similar behaviour is shown by other theoretical models for absorption spectra [16, 17]. In order to understand another characteristic of the FES in both types of system we take, in the following, an infinite mass for the hole.

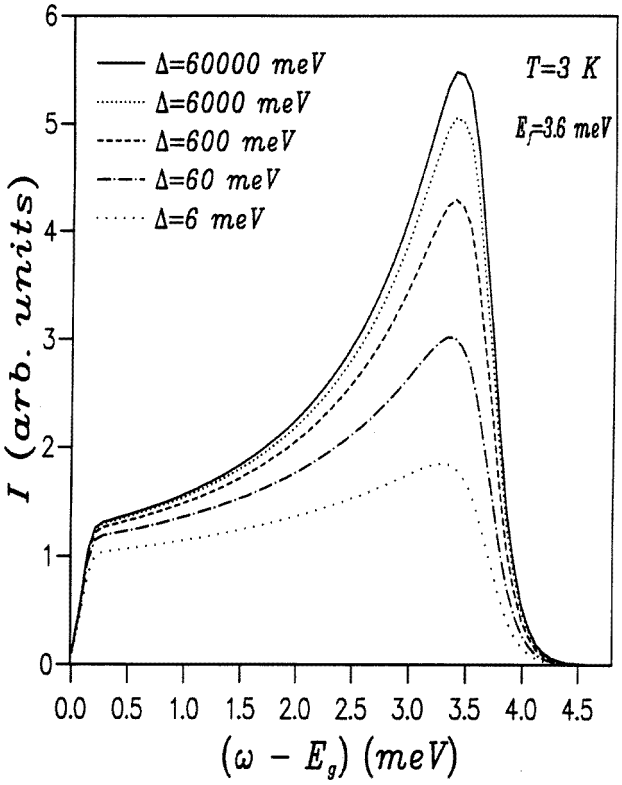

Figure 2. Emission spectra of direct quantum wells for different intrasubband separations for $E_F = 3.6$ meV, $m_h \to \infty$ and temperature $T = 3$ K.

3.1. Direct systems

3.1.1. The confining potential. In this section we study how a FES is affected by electronic confinement in the z-direction. We first consider the behaviour of a direct system, with the same parameters as in figure 1, when the system goes from being a purely 2D system to

being a Q3D system, i.e. from $\Delta \to \infty$ to a finite value of Δ. The well width varies according to the variation of Δ. Our results in figure 2 show that when the width of the well is increased, i.e., a Q3D system in terms of Coulomb interaction, the electron–hole interaction decreases, due to a form factor less than one, and therefore the FES is strongly suppressed. For values $\Delta > E_F$, the FES is more evident in 2D systems than in Q3D systems. Therefore, in these direct systems, the FES is lower in intensity when the second subband is close to the top of the Fermi level. Due to the symmetry of the system it is possible to have transitions between even- or odd-parity electron bands, but they never interfere with each other, even in the case where $E_F > \Delta$.

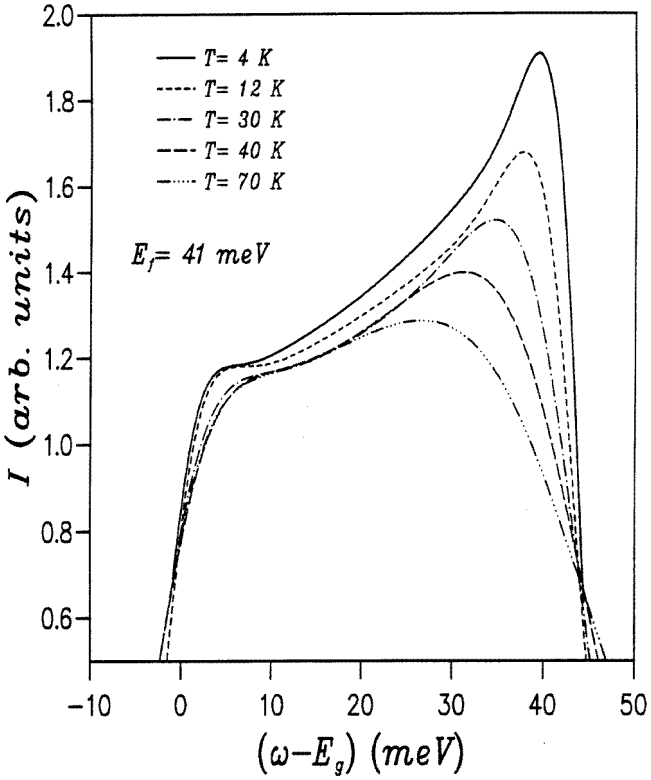

Figure 3. Emission spectra of direct quantum wells for different temperatures. $E_F = 41$ meV, $m_h \to \infty$ and $\Delta \to \infty$.

3.1.2. Temperature effects. In figure 3 we show the emission spectrum for different values of temperature and for a high electron density, $E_F = 41$ meV, which corresponds to a two-dimensional density of $n \approx 1 \times 10^{12}$ cm^{-2}. In this case, electrons thermally excited to the next subband do not play an important role, so we will limit ourselves to considering just electron–hole correlations at the Fermi level. The main effect produced by electron–electron interaction is the appearance of the FES. Neglecting many-body effects, and for low temperatures, the emission spectra would be given by the convolution of the two-dimensional electron and hole densities of states multiplied by their respective Fermi functions. The luminescence lineshape would correspond to the steplike 2D joint density of states, with total width given by E_F, since the chemical potential of holes is zero.

For low temperatures the peak of the FES is stronger than for the high-temperature case [11]. The peak at the Fermi edge begins to decrease in intensity when the temperature is increased up to 40 K. At this temperature the electron correlations are diminished as a consequence of the broadening at the Fermi edge. When the temperature is further increased to 70 K the spectra only show a shoulder associated with the remainder of the FES. At temperatures of the order of the exciton binding energy E_0 we see that many-body effects do not significantly affect the spectrum at the Fermi level. We believe that this peak must be even lower in intensity, because the effects of temperature were considered in the non-interacting electron–hole Green function but not in the polarizability of the screened Coulomb interaction. In order to obtain a more quantitative agreement with the experimental results it is necessary to include temperature effects both in the screened interaction as well as in the hole spectral function. However, these features should not drastically change the physics associated with the FES and their inclusion will make the theoretical treatment much more cumbersome.

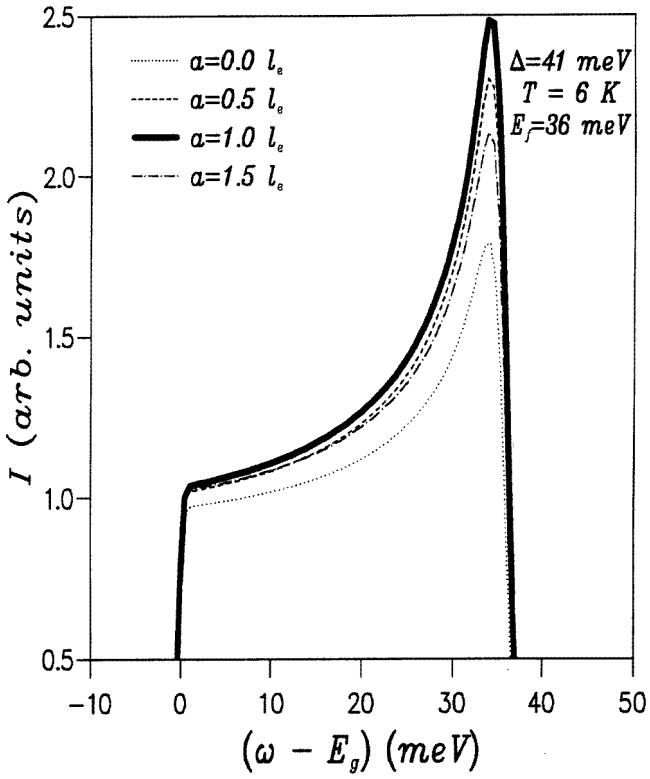

Figure 4. The emission spectrum in indirect doped quantum wells for different electron–hole separations a. $T = 6$ K, $E_F = 36$ meV, $\Delta = 41$ meV and $m_h = 10\,000 m_e^*$.

3.2. Indirect systems

3.2.1. Effects of broken symmetry. Heretofore our results have been for a single DPQW with electrons and holes coexisting in the same spatial region. The luminescence spectrum changes if this condition is broken, because the symmetry and selection rules are different

when the 2DEG and the hole no longer coexist in the same spatial region. The luminescence spectrum calculated as a function of the electron–hole separation a is shown in figure 4. We have taken the same parameters as for the experiment described in [12], $E_F = 36$ meV, $T = 6$ K, $\Delta = 41$ meV. We suppose a dispersionless hole ($m_h = 10\,000 m_e^*$) due to impurities, potential fluctuations, etc.

Firstly, we consider the case in which the effects arising from electrons excited to the second subband are not very important. A difference in energy from the Fermi level to the bottom of the second conduction subband of 5 meV has been considered. In this case we observe that the breaking of symmetry in the problem leads to an enhancement at the Fermi edge, as compared with the symmetric case, $a = 0$ nm. The contribution $G_{01;01}$ (22), arising from virtual transitions from the Fermi edge to the second subband, is not crucial because of the large interband separation Δ. This allows us to restrict our study to the effects arising from the a-separation over the FES. The maximum value of the FES is obtained when $a \approx l_e$, i.e., the hole attains the maximum probability amplitude at the edge of the electron well.

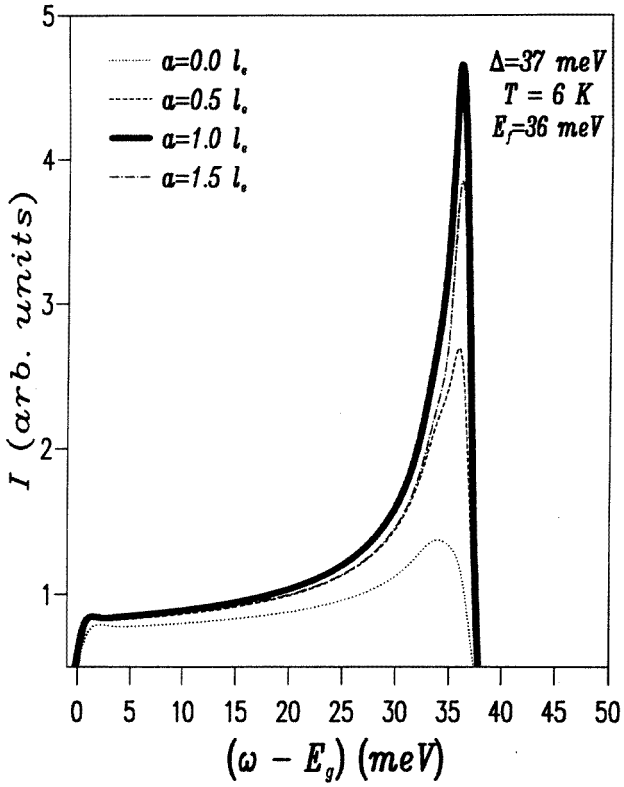

Figure 5. The emission spectrum of indirect quantum wells for varying electron–hole separation a. $T = 6$ K, $E_F = 36$ meV, $m_h = 10\,000 m_e^*$ and $\Delta = 37$ meV. The resonance at the Fermi edge is increased without having thermally excited electrons populating the second subband.

The monoelectronic wavefunctions of the c_1 and c_2 conduction subbands have different spatial extensions in the z-direction and consequently different overlaps with the hole wavefunction. For $q \approx 0$ our results show that the interactions $V^{(s)}_{0,1;0,1} > V^{(s)}_{0,0;0,0}$ just when $a \to l_e$. For this value of a, the interband term is greater as $q \to \pm k_F$, which is the

most important region for computing the interacting electron–hole Green function. This is due to the fact that overlapping between the monoelectronic functions from the electrons in the second subband is greater than that of the first electronic subband with the hole. It will be reflected in the response function through the coupling between electron states with $q = \pm k_F$ and electron states with $q = 0$, opening up a new resonant scattering channel and producing an increase in the luminescence signal at the Fermi edge [15, 19, 20, 22, 38].

Intraband interactions, obviously, decrease when the separation distance a is further increased. The intrasubband transitions given in (22) by the symmetric propagators, $G_{00;10}+G_{01;00}$, are different from zero and contribute to the spectrum. Our results show that the FES, coming from low-energy excitations at the Fermi edge, can be coupled to virtual transitions through a new scattering channel, the bottom of the second subband, increasing the luminescence signal at the Fermi edge [12, 21, 22]. In the direct case, these terms are zero, so the mixing does not occur and the contribution of a new channel that couples the FES with a resonant state cannot be invoked.

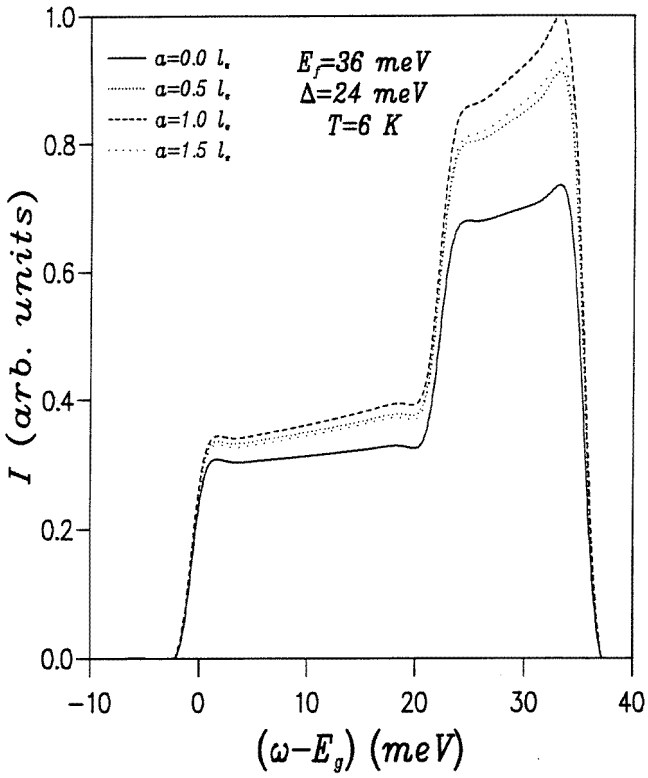

Figure 6. The luminescence spectrum of indirect quantum wells for different electron–hole separations a. $T = 6$ K, $E_F = 36$ meV, $m_h = 10\,000 m_e^*$ and $\Delta = 24$ meV, so the second conduction subband is populated by free carriers.

In order to clarify the effect of this new channel we change the width of the well in the z-direction, i.e. we move the bottom of the second electronic subband with respect to the Fermi edge. As we show in figure 5, when the separation between the Fermi edge and the bottom of the second conduction subband is 1 meV we can observe that the resonance at the Fermi edge clearly increases. The main contribution to the spectrum comes from

the $G_{00;10} + G_{01;00}$ terms which are the responsible for the mixing of the v–c_2 resonance with excitations of the Fermi sea. Therefore, a strong resonant coupling between the v–c_2 transition and the FES in a 2DEG is shown in the luminescence spectrum [12]. This behaviour is similar to that in the case in which the second subband is really populated by free carriers. This case is shown in figure 6 where we take $\Delta = 24$ meV. Dipole matrix elements have been taken as constant because they do not qualitatively change the physics of the system [39]. In this case two singularities appear arising from the first and second Fermi wavevectors in each conduction subband. Our results show clearly that the FES arises only from low-energy excitations at the Fermi edge and also that it can be increased in *indirect* systems, if the intraband separation is reduced. In this case, the low-energy excitations, or electron–hole pairs, have a high probability of mixing with excitations coming from electrons in the second subband. It is worth nothing that these transitions are virtual, and that the coupling of the FES to resonances can be an efficient mechanism for controlling the luminescence enhancement at the Fermi level.

The final result is that the intensity of the FES in indirect systems for finite q is stronger than in the direct case and clearly explains the importance of a vicinal conduction subband.

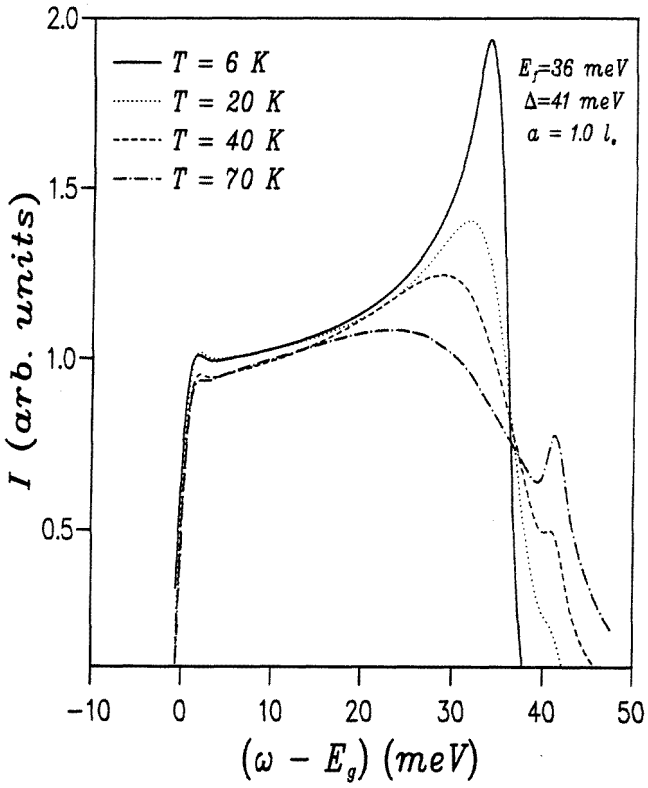

Figure 7. The emission spectrum of indirect quantum wells for $a = l_e$ at different temperature values: $T = 6$ K (continuous line); $T = 20$ K (dotted line); $T = 40$ K (dashed line); $T = 70$ K (chain line). The second peak corresponds to transitions of electrons thermally excited to the next conduction subband. $E_F = 36$ meV, $m_h = 10\,000 m_e^*$ and $\Delta = 41$ meV.

3.2.2. Temperature effects. In figure 7 we show the luminescence spectrum for different temperatures. The results are shown for experimental parameters [20] $E_F = 36$ meV and $\Delta = 41$ meV, and for the most favourable situation for obtaining a strong FES, $a \approx l_e$. The FES as well as in the symmetric case disappears for $T \approx 40$ K. When the temperature is roughly the difference between the bottom of the second conduction subband and the Fermi edge, the spectrum shows a second peak above the previous FES. This peak arises from transitions of electrons thermally excited to the second conduction subband, showing typical behaviour of QW spectra [11, 20, 38, 40]. When the width well is increased and the temperature is raised the spectrum is dominated by transitions to the second subband and the FES decreases. This again agrees with the experimental temperature dependence.

In general when our results are compared with the experimental situation we find a satisfactory qualitative agreement. This supports the ladder approximation as being adequate for studying the experimental spectra under low-power optical excitation, where quasi-equilibrium systems should be considered.

4. Conclusions

Summarizing the results obtained, we have studied the luminescence spectra of direct and indirect doped quantum wells with a parabolic confinement. We use a three-subband model within the ladder approach for the spectra and the RPA approach for the screening response of the electron Fermi sea. The luminescence spectrum is studied as a function of the temperature, width of the well and effective mass for the hole. It is possible to observe FESs in these systems, when one condition is fulfilled: that of an infinite mass for the hole. This condition is physically justified as being due to potential fluctuations, impurities, etc. The FES is easier to observe in Q2D systems than in Q1D or Q3D systems due to the decrease of the joint density of states and the confinement potential, respectively. At temperatures of 60 K the Fermi surface is broadened and the electron correlations diminish, so the FES is quenched.

For indirect systems, spatial symmetry breaking produces important effects in the luminescence spectrum. This spatial breaking of symmetry implies that all transitions are allowed. According to the spatial separation between the 2DEG and the hole we found that the electron coupling between electrons coming from the first and second subband presents a maximum for $a \approx l_e$. This characteristic allows the resonant mixing between the states at the Fermi level and virtual transitions to the next conduction subband. Therefore an enhancement in the luminescence signal is observed. For direct and indirect systems the temperatures at which the FESs disappear are similar. Even when a thermal population of electrons in the second subband exists, transitions of these electrons do not contribute to the enhancement of the FES. The main result is that the FES is stronger in indirect than in direct systems due to the fact that a new scattering channel is opened. We must stress that our approach is valid only in situations close to equilibrium.

Acknowledgments

We are grateful to L Quiroga for useful discussions and the critical reading of the manuscript, and to J J Dorado for his help. This work was supported in part by the Comision Interministerial de Ciencia y Tecnologia of Spain under contract MAT 94-0982-C02-01, the European Community under contract ESPRIT.BRA 6719 (NANOPT) and the Ministerio de Educación y Ciencia of Spain under Programa de Cooperación Cientifica con Iberoamérica.

One of us (FJR) acknowledges COLCIENCIAS of Colombia for financial support under contract No 1204-05-264-94.

References

[1] Pinczuk A, Shah J, Miller R C, Gossard A C and Wiegmann W 1984 *Solid State Commun.* **50** 735
[2] Paquet D, Rice T M and Ueda K 1985 *Phys. Rev.* B **32** 5208
[3] Skolnick M S, Whittaker M, Simmonds P E, Fischer T A, Saker M K, Rorison J M, Smith R S, Kirby P B and White C R H 1991 *Phys. Rev.* B **43** 7354
[4] Chen W, Fritze M, Nurmikko A V, Hong M and Chang L L 1991 *Phys. Rev.* B **43** 14 738
[5] Zhang Y H and Ploog K 1992 *Phys. Rev.* B **45** 14 069
[6] Folkes P A, Dutta M, Rudin S, Shen H, Zhou W, Doran D S, Taysing-Lara M, Newman P and Cole M 1993 *Phys. Rev. Lett.* **71** 3379
[7] Ding J, Hagerott M, Kelkar P, Nurmikko A V, Grillo D C, He L, Han J and Gunshor R L 1994 *Phys. Rev.* B **50** 5787
[8] Smith P M, Chao P C, Ballingal J M and Swanson A W 1990 *Microwave J.* **33** 71
[9] Shayegan M, Jo J, Suen W, Santos M and Goldues V J 1990 *Phys. Rev. Lett.* **65** 2916
[10] Rorison J M 1987 *J. Phys. C: Solid State Phys.* **20** L311
[11] Skolnick M S, Rorison J M, Nash K J, Mowbray D J, Tapster P R, Bass S J and Pitt A D 1987 *Phys. Rev. Lett.* **58** 2130
[12] Chen W, Fritze M, Walecki W, Nurmikko A V, Ackley D, Hong J M and Chang L L 1992 *Phys. Rev.* B **45** 8464
[13] Mueller J F 1990 *Phys. Rev.* B **42** 11 189
Mueller J F, Ruckenstein A E and Schmitt-Rink S 1990 *Mod. Phys. Lett.* **5** 135
[14] Hawrylak P 1992 *Solid State Commun.* **81** 525
[15] Nash K J, Skolnick M S, Saker M K and Bass S J 1993 *Phys. Rev. Lett.* **70** 3115
[16] Uenoyama T and Sham L J 1990 *Phys. Rev. Lett.* **65** 1048
[17] Hawrylak P 1991 *Phys. Rev.* B **44** 3821
[18] Bauer G E W 1992 *Phys. Rev.* B **45** 9153
[19] Fritze M, Chen W, Nurmikko A V, Jo J, Santos M and Shayegan M 1992 *Phys. Rev.* B **45** 8408
[20] Fritze M, Chen W, Nurmikko A V, Jo J, Santos M and Shayegan M 1993 *Phys. Rev.* B **48** 15 103
[21] Chen W, Fritze M, Nurmikko A V, Ackley D, Colvard C and Lee H 1990 *Phys. Rev. Lett.* **64** 2434
[22] Wagner J, Ruiz A and Ploog K 1991 *Phys. Rev.* B **43** 12 134
[23] Schmitt-Rink S, Chemla D S and Miller D A B 1989 *Adv. Phys.* **38** 89
[24] Rodriguez F J and Tejedor C 1993 *Phys. Rev.* B **47** 1506
[25] Combescot M and Tanguy C 1994 *Phys. Rev.* B **50** 11 484
Tanguy C and Combescot M 1994 *Phys. Rev.* B **50** 11 499
[26] Keldysh L V 1965 *Sov. Phys.–JETP* **20** 1018
[27] Mahan G D 1967 *Phys. Rev.* **153** 882; 1967 *Phys. Rev.* **163** 612
[28] Nozières P and Dominicis C T 1969 *Phys. Rev.* **178** 1097
[29] Ohtaka K and Tanabe Y 1990 *Rev. Mod. Phys.* **62** 929
[30] Hawrylak P 1990 *Phys. Rev.* B **42** 8986
[31] Rodriguez F J 1994 *PhD Thesis* Universidad Autónoma de Madrid
[32] Gradshteyn I S and Ryzhik I M 1965 *Table of Integrals Series and Products* 4th edn (New York: Academic)
[33] Tejedor C and Rodriguez F J 1993 *Frontiers of Optical Phenomena in Semiconductor Structures of Reduced Dimensions* ed D J Lockwood and A Pinczuk (Dordrecht: Kluwer Academic)
[34] Rodriguez F J and Tejedor C 1993 *Phys. Rev.* B **47** 13 015
[35] Calleja J M, Goni A R, Denis B S, Weiner J S, Pinczuk A, Schmitt-Rink S, Pfeiffer L N, West K W, Mueller J F and Ruckenstein A E 1991 *Solid State Commun.* **79** 911; 1992 *Surf. Sci.* **263** 346
[36] Penna A F S, Shah J, Pinczuk A, Sivco D and Cho A Y 1985 *Appl. Phys. Lett.* **46** 184
[37] Cingolani R, Stolz W, Zhang Y H and Ploog K 1990 *J. Lumin.* **46** 147
[38] Fisher T A, Simmonds P E, Skolnick M S, Martin A D and Smith R S 1993 *Phys. Rev.* B **48** 14 253
[39] Moreover the matrix elements of the momentum should be very small for large a, diminishing any possible remainder of the singularity.
[40] Gumbs G, Huang D, Yin Y, Qiang H, Yan D and Pollak F H 1993 *Phys. Rev.* B **48** 18 328